Quaternary Geochronology 40 (2017) 109–119

Contents lists available at ScienceDirect

Quaternary Geochronology

journal homepage: www.elsevier.com/locate/quageo

The first tephra evidence for a Late Glacial explosive volcanic eruption in the Arxan-Chaihe volcanic field (ACVF), northeast China

Chunqing Sun [a, b, *], Qiang Liu [a], Jing Wu [a], Károly Németh [c], Luo Wang [a], Yongwei Zhao [d], Guoqiang Chu [a], Jiaqi Liu [a]

[a] *Key Laboratory of Cenozoic Geology and Environment, Institute of Geology and Geophysics, Chinese Academy of Sciences, Beijing, 100029, China*
[b] *University of Chinese Academy of Sciences, Beijing, 100049, China*
[c] *Institute of Agriculture and Environment, Massey University, Palmerston North, New Zealand*
[d] *Institute of Geology, China Earthquake Administration, Beijing, 100029, China*

ARTICLE INFO

Article history:
Received 2 February 2016
Received in revised form
11 October 2016
Accepted 17 October 2016
Available online 18 October 2016

Keywords:
Tephra
Tephrochronology
Arxan-Chaihe
Northeast China
Greater Khingan Mountains
Moon lake
Late Glacial

ABSTRACT

A 5 mm thick tephra layer has been identified in the lacustrine sediments of Moon Lake in the Arxan-Chaihe volcanic field (ACVF) in Greater Khingan Mountains (NE China). The visible tephra layer is clearly revealed as a distinct peak in magnetic susceptibility measurements. The tephra layer consists mainly of brown vesicular glass shards and minor amounts of plagioclase, olivine and clinopyroxene. Major and minor element analysis has been carried out on the glass shards and plagioclase minerals. Glass shards show low concentrations of K_2O, similar to the eruptive products derived from post-Miocene volcanoes of the ACVF. The plagioclase phenocrysts in both lava and tephra from ACVF, and in the tephra recorded in Moon Lake are labradorites. During the Late Pleistocene to Holocene, there were also extensive explosive eruptions in the nearby Nuominhe volcanic field (NVF). Volcanic rocks from the ACVF are easily distinguished from those derived from the NVF, having distinctly different K_2O concentrations. This compositional variation is likely the result of different magmatic processes operating in the ACVF and NVF. Radiocarbon dating on organic materials from the lacustrine sediments dates the tephra layer to ca. 14,200 cal yrs BP, which implies that it was generated by a previously unknown Late Pleistocene explosive eruption in the ACVF. These results, for the first time, give a direct tephra record in this area, and suggest that identification of further tephra and/or cryptotephra in local sedimentary basins such as crater lakes of scoria cones and maars will be significant for dating the Late Pleistocene to Holocene volcanic eruptions and will help to establish a detailed record of the volcanic activity in the ACVF. The newly discovered tephra layer also provides a dated tephrochronological marker layer, which will in future studies provide a means to synchronise local sedimentary records of the climatically variable Late Glacial.

1. Introduction

Volcanic ash produced during explosive eruptions can be transported and deposited over extensive areas, providing excellent isochronous maker layers. Tephra layers have been successfully used to correlate and link Quaternary events, providing tools for reconstructing records of Quaternary volcanic activity, estimating environmental impacts on human evolution, and synchronising climatic and environmental changes across a certain area (Albert et al., 2013; Lane et al., 2013a, 2013b; Lowe, 2011; Lowe et al., 2012; Molloy et al., 2009). Additionally, well-dated tephra layers can be used to constrain and refine the age-depth information of the sediments where the tephra layers are detected. Alternatively, if the age of the tephra is unknown, but the age of the host sediment is well constrained, the latter can be used to date the tephra layer/eruptive event (Coulter et al., 2012; Sun et al., 2014a). In recent years, various projects related to tephrochronology have been carried out around Europe and other areas, such as INTIMATE (Integration of ice core, marine, and terrestrial records: refining the record of the last glacial interglacial transition), RESET (Response of humans to abrupt environmental transitions) and PASADO (Potrok

* Corresponding author. Key Laboratory of Cenozoic Geology and Environment, Institute of Geology and Geophysics, Chinese Academy of Sciences, Beijing, 100029, China.
E-mail address: suncq@mail.iggcas.ac.cn (C. Sun).

http://dx.doi.org/10.1016/j.quageo.2016.10.003
1871-1014/

Aike maar lake Sediment Archive Drilling prOject) (Davies et al., 2004; Lowe et al., 2008, 2012; Zolitschka et al., 2013). In addition, tephra layers invisible to the naked eye, known as cryptotephra, may be detected and separated from sedimentary records hundreds or thousands of kilometres from the volcanic source, which dramatically extends the application of tephrochronology (Davies, 2015; Lowe, 2011). Therefore, tephrochronology is becoming more and more significant for temporally constraining our understanding of environmental and climate changes during the Quaternary; whilst also refining the eruptive histories of less well-studied Quaternary volcanic fields.

During the Cenozoic, there were extensive volcanic eruptions in the northeast China as a response to the subduction of the Pacific plate (Liu, 1999; Liu et al., 2001). In northeast China, six major volcanic regions can be identified including Changbaishan volcano and the Longgang, Jingbohu, Nuominhe (NVF), and Arxan-Chaihe (ACVF) volcanic fields (Fig. 1). Changbaishan volcano and the nearby Longgang and Jingbohu volcanic fields, are located more than 700 km east of ACVF. Two additional post-Miocene volcanic fields lie to the northeast of the ACVF: Nuominhe (NVF, ~300 km away) and Wudalianchi (NVF, ~500 km away).

In the ACVF, many volcanic cones with widespread long lava flows and pyroclastic deposits, display seemingly youthful morphologies. Fresh lava flow surface morphologies are exposed perfectly in numerous locations, with zero or only minimal sediment and vegetation cover. In previous studies, the idea that most volcanoes of the ACVF erupted during the Late Pleistocene and Holocene has been argued based solely on these well-preserved morphologies, whilst almost no detailed geochronological or geochemical evidence has been provided (e.g. Bai et al., 2005). The geothermal activity in the ACVF is also very strong, indicating a potential shallow magmatic heat source. The local Budong River is so named because it cannot be frozen even in cold winters, due to the subsurface geothermal activity. The apparent young age and current geothermal activity of the ACVF means that developing a detailed volcanic history and understanding of the evolution is essential for assessing future volcanic hazards in the region.

Lakes and peatlands in and around volcanic fields can provide depositories for tephra layers, which make it possible to date the Late Pleistocene to Holocene eruptions based on the age of their host sediments. However, in comparison to, for example, European areas, tephrochronological studies in China are not very common. This is especially the case in the ACVF (Fig. 1), where in addition, basic volcanological research is also rare. This is partially due to difficulties in accessing the area and the poor outcrop conditions caused by thick continental woodland cover across the region (Zhao et al., 2013). Consequently, many volcanoes in the ACVF have no formal names and are instead termed "*#### high land volcano*", e.g. the "*1381 high land volcano*" (Fig. 1).

To date, only a few radiometric age determinations have been performed successfully on pre-Holocene eruptions using K-Ar methods. Geochronological studies have been supplemented by

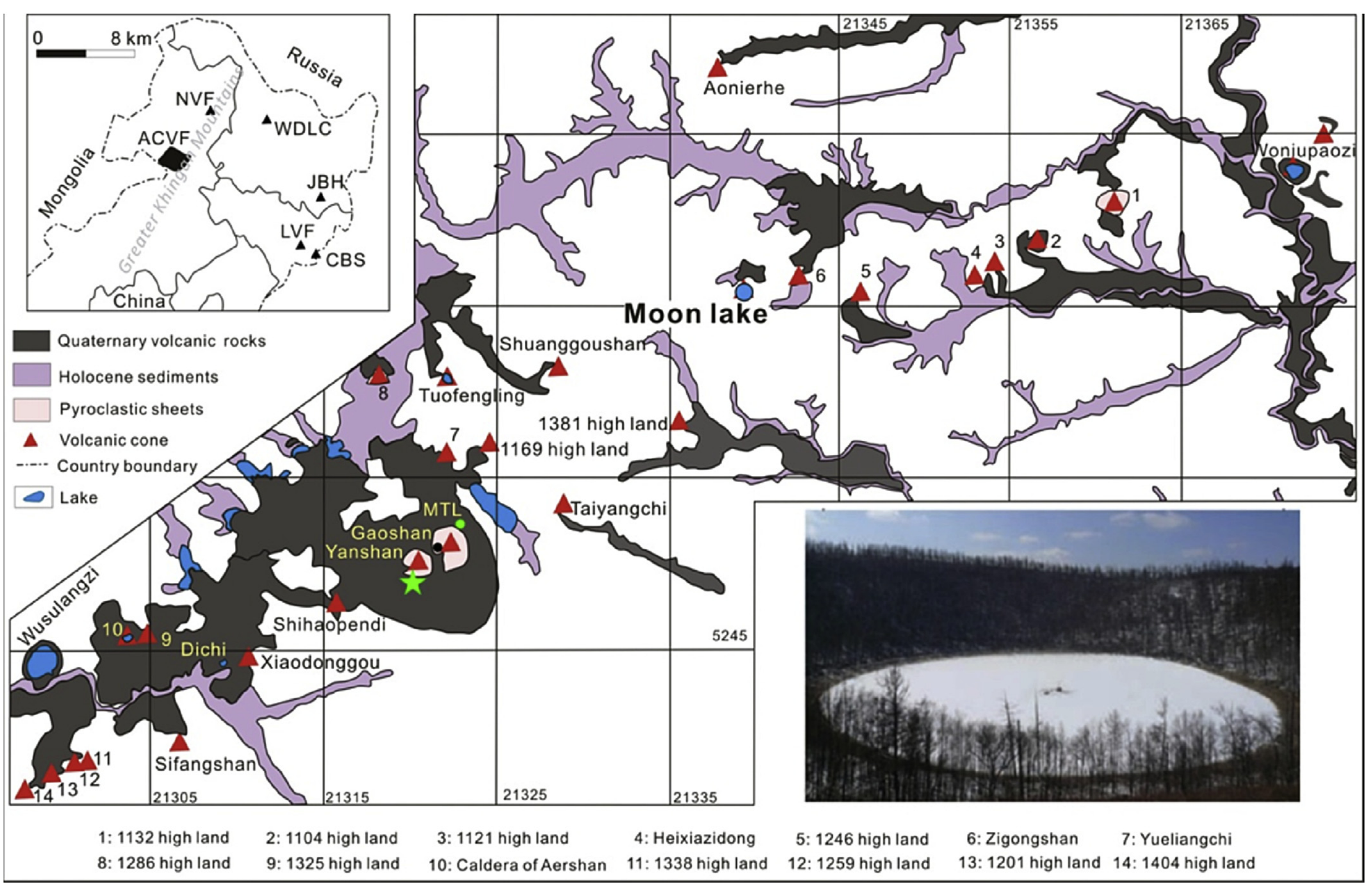

Fig. 1. Map of the volcanic geology and distribution of lakes within the Arxan-Chaihe volcanic field (ACVF). Insert map (modified from Zhao et al. (2008)) shows the location of other volcanic fields (Nuominhe (NVF), Wudalianchi (WDLC), Longgang (LVF), Jingbohu (JBH), and Changbaishan (CBS) volcanic fields) referred to in the text. Insert photo shows Moon Lake. The green star marks the location where charcoals were dated to 2000 cal yrs BP by Bai et al. (2005). MTL is the main reported peat site in ACVF. The known volcanic cones in the ACVF are numbered 1–14. The black solid circle marks the proximal tephra sample site near Gaoshan volcano. (For interpretation of the references to colour in this figure legend, the reader is referred to the web version of this article.)

further analytical data, such as whole rock geochemistry and geophysical data, in order to understand the petrogenesis and magma chamber processes associated with the dated sites (e.g. Fan et al., 2011; Liu, 1987; Tang et al., 2005; Zhao and Fan, 2012). So far however, no research on proximal pyroclastic deposits, or distal tephra, have been carried out in this field. Hence, there is no volcanic glass or mineral chemistry data known from pyroclastic successions in the ACVF that could be used for correlating proximal and distal tephra deposits. The lack of information makes it difficult to establish a reliable order of volcanic events since the Pleistocene in the ACVF.

The ACVF is located at the current northern limit of the East Asian monsoon, and it is a very sensitive region to climate changes. $\delta^{13}C_{org}$, pollen, and charcoal records from high resolution lake sediments archives have been used to constrain vegetation evolution and climate changes (Liu et al., 2010; Wu and Liu, 2012, 2013; Wu et al., 2016). The Greater Khingan Mountains are one of three main peatlands in China (Fig. 1), and the ACVF is home to the most important peat site in the mountain range (Bao, 2012). Peat core sequences in the region have been used to characterise atmospheric dusts sources based on the geochemical composition of peat samples (Bao et al., 2012, 2015 and references therein), and to deduce modern climate and vegetation changes based on cellulose $\delta^{13}C_{org}$ and *n*-Alkanes-inferred climate reconstructions (Lin et al., 2004; Zhang et al., 2014). Despite the diversity of sedimentary contexts and the evidence for many volcanic eruptions in this region, no tephra or cryptotephra studies have been previously performed on lake or peat sediments in order to resolve the timing of volcanic eruptions, or to link the climatic changes recorded within the numerous sedimentary records.

This study presents the first geochemical and geochronological investigation of a tephra layer recorded in lake sediments from ACVF, northeast China. These new findings provide a marker bed for linking rapid climatic events in this region during the Late Glacial and evidence an explosive eruption, offering new insights into the volcanic history of the region during the Late Pleistocene. In addition, we demonstrate that further tephra or cryptotephra studies in similar sedimentary contexts will provide an excellent means to date and decipher past (e.g. Late Pleistocene to Holocene) volcanic activity in the ACVF, which is significant for the forecasting of future volcanic hazards.

2. Geological background

The Arxan-Chaihe volcanic field (ACVF), covers an area of ~1000 km^2 in the middle segment of the Greater Khingan Mountains where about 30 volcanic edifices are preserved (Fig. 1). The volcanic rocks of the ACVF consist predominantly of extensive pahoehoe to aa-type basaltic lava flows, as well as variously indurated phreatomagmatic and magmatic pyroclastic deposits, commonly associated with widespread pyroclastic fall deposits (Bai et al., 2005; Fan et al., 2008; Zhao and Fan, 2010; Zhao et al., 2008). The source volcanoes of these volcanic products show an southwest-northeast alignment (Fig. 1). The Cenozoic volcanic rocks are mainly alkali basaltic rocks, which immediately overlie the Mesozoic crystalline basement. Volcanic activity started since the Pliocene and is inferred to have been most extensive during the Mid Pleistocene, decreasing in frequency during the Late Pleistocene and Holocene (Zhao, 2010). Gaoshan and Yanshan volcanoes are thought to have the youngest eruptions dated at c. 2000 cal yrs BP, according to AMS ^{14}C dating of charcoals in pyroclastic deposits of Yanshan volcano (Bai et al., 2005). The relatively short distance to the NVF, where numerous explosive eruptions occurred during the Late Pleistocene to Holocene, mean that the NVF could also be a source of tephra or cryptotephra layers in ACVF.

In the ACVF there are various types of lakes and peat bogs formed by volcanic activities (Zhao, 2010; Zhao et al., 2008). These include: i. maar lakes, such as the Woniupaozi maar (Fig. 1); ii. crater lakes of scoria cones, such as the Moon Lake; iii. many shallow lava flow dammed lakes, formed in front of young lava flows; and iv. lakes that formed by pahoehoe lava flow tube roof collapse and subsequent water infill, such as the Dichi Lake. Most of these lakes have a stable depositional environment because there are no inflows and outflows of streams; the primary sources of water are groundwater and rainfall; and they have experienced no major impacts due to human activity (Liu et al., 2010). The undisturbed sedimentary conditions make these volcanic lakes perfect sites to investigate eruption chronologies and construct tephrostratigraphies.

Moon Lake, in the ACVF (47°30′25″N, 120°52′05″E, altitude at water level 1190 m.a.s.l), is a small crater lake just 0.19 km in diameter and with a maximum water depth of 6.5 m (Fig. 1). The mode of formation of Moon Lake is not entirely known. Limited research has been conducted into the eruptive history of this volcanic edifice (Zhao, 2010), therefore for clarity we here refer to the lake as a crater lake to be consistent with definitions used elsewhere (e.g. Christenson et al., 2015). As the lake lies on a crater enclosed in a positive landform, which is primarily composed of scoriaceous pyroclastic deposits, we infer that the lake formed in a scoria cone crater that was sealed at some stage, preventing water escape. While similar scoria cone-hosted lakes are known elsewhere in humid climate regions (e.g. in top of many Pacific Islands such as Samoa (Németh and Cronin, 2009)), the oval shape in map view and the relatively low rim-to-crater diameter ratio, suggest that it might be part of either a fissure-aligned vent system or may there may have been some direct phreatomagmatic explosive excavation during its evolution. Further research on the origin of the Moon Lake remains to be conducted to confirm the volcanic processes responsible for the crater formation.

3. Materials and methods

Sedimentary cores were taken using a piston corer in the centre of the Moon Lake in March 2007. The total length of the profile collected is about 9 m and the detailed lithological components have been described by Liu et al. (2010). Low-frequency volumetric magnetic susceptibility measurements were carried out on 1 cm contiguous samples (Fig. 2) using a MS2B magnetic susceptibility meter (Bartington) in the Paleomagnetism and Geochronology Laboratory (PGL), at the Institute of Geology and Geophysics, Chinese Academy of Sciences.

The most recent activity from the area of the Gaoshan and Yanshan volcanoes has been divided into two stages; the first stage is an explosive eruption that produced extensive scoriaceous fallout pyroclastic deposits, while the second emitted lava flows that entered into and partially diverted the syn-eruptive fluvial network (Bai et al., 2005; Zhao and Fan, 2010). These two volcanoes are also the highest volcanic cones in the ACVF, with Gaoshan cone reaching c. 362 ma.s.l. and Yanshan c. 233 m.a.s.l.. As part of this study, proximal tephra samples from the Gaoshan and Yanshan deposits were collected in the field at the ACVF pyroclastic sheet for comparison of the chemical composition with those of the ash samples recovered from the Moon Lake in this study.

Samples from peaks of magnetic susceptibility were treated with 10% HCl to remove carbonates and with H_2O_2 to remove organic materials. Samples were then sieved, and particles between 30 μm and 100 μm were kept and checked for the presence of glass particles under the microscope. Pure glass shards and phenocrysts were picked up under the microscope, and then mounted and polished to expose the internal sections for electron microprobe analysis (EPMA).

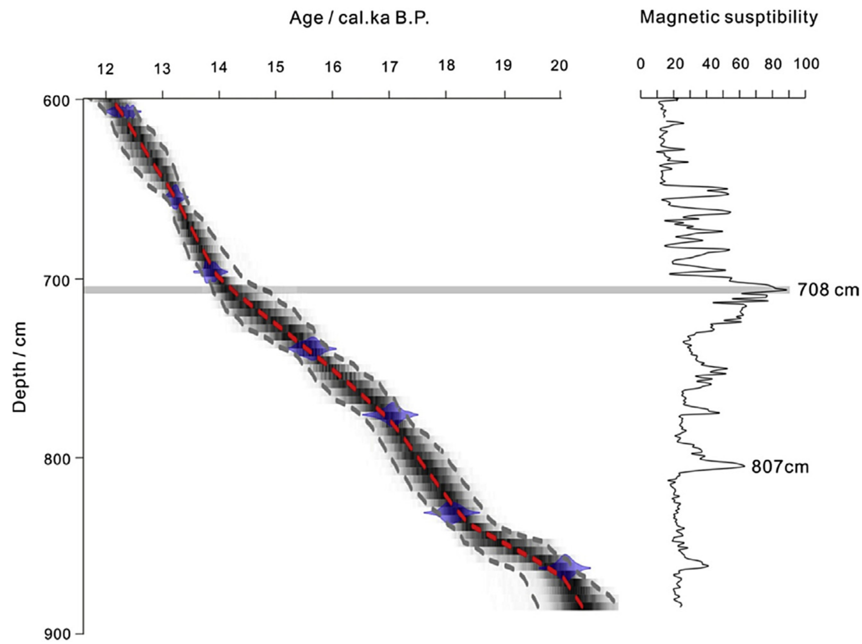

Fig. 2. Age-depth model (age estimates from Liu et al. (2010)) and magnetic susceptibility of the Moon Lake sediment core. Tephra layer ML 708 is located at the position of the highest level of magnetic susceptibility, indicated by the horizontal grey line.

In situ major element analysis on tephra glass shards by EPMA is the most widely used method to characterise and correlate tephra layers (e.g. Lane et al., 2011, 2013a, b; Lowe, 2011; Plunkett et al., 2015) due to the fact that bulk tephra samples usually contain mineral and lithic components not equally represented in more distal tephra deposits (Shane et al., 2008). In some cases, the major and minor element composition of minerals (e.g. plagioclase, biotite and Fe-Ti oxides) or/and the trace element composition of glass shards, can give additional evidence leading to more reliable correlation of tephra layers to their source volcanoes (Jouannic et al., 2015; Pearce et al., 2004a, b; Shane, 1998; Smith et al., 2011; Sun et al., 2016). In this study, the major and minor element compositions of plagioclase minerals from Moon Lake tephra were also determined by EPMA using the same instrumental set up as for glass shards.

EPMA, using a wavelength-dispersive spectrometer (WDS) was performed on a JEOL JXA 8100 electron microprobe at the State Key Laboratory of Lithospheric Evolution, Institute of Geology and Geophysics, Chinese Academy of Sciences. In order to ensure comparative datasets, glass compositions for proximal tephra samples from the ACVF were also analysed using the same instrument and analytical conditions. Nine major and minor elements (Na, Mg, Al, Si, K, Ca, Fe, Ti, Mn) were analysed with an accelerating voltage of 15 kV, a beam current of 6 nA, and a beam diameter of 10 μm. Peak counting times used were 20 s for all elements except for Na (10 s). The measurement of Na content was made at the start of analysis. Secondary standard glasses from the MPI-DING fused glass ML3B-G (Jochum et al., 2006) was used to monitor the precision and accuracy of the data. During analysis of glass shards, 2–3 spots were analysed on a single shard to see if they were heterogeneous in composition within a single glass shard.

4. Results

Identified magnetic susceptibility peaks (at 194, 545, 708 and 807 cm) were investigated, however only that at 708 cm contained tephra. The tephra layer at around 708 cm consists of volcanic glass shards, plagioclase, pyroxene and olivine. The tephra layer (ML 708) is visible to the naked eye and its thickness is approximately 5 mm. The glass shards have abundant bubbles and sharp edges (Fig. 3) illustrating no obvious secondary depositional processes have

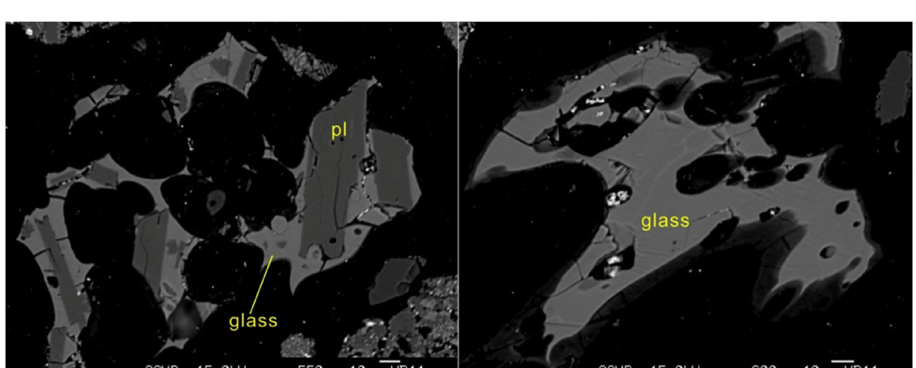

Fig. 3. Back scattering electron (BSE) map of glass shards (glass) and plagioclase (pl) minerals from Moon Lake tephra ML 708.

Table 1
WDS-EPMA major and minor element composition of glass shards for the tephra from Moon Lake. All the data have been normalised to an anhydrous basis with original analytical totals shown. MPI-DING glass standard ML3B-G was analysed to monitor the precision and accuracy of the glass data.

	SiO_2	TiO_2	Al_2O_3	FeO	MnO	MgO	CaO	Na_2O	K_2O	Analytical total
ML 708	51.37	2.41	14.89	10.38	0.14	5.31	10.31	3.72	1.46	97.32
	51.23	2.34	15.68	10.45	0.19	4.82	9.85	3.78	1.67	97.33
	51.05	2.63	15.57	10.61	0.16	4.68	9.77	3.72	1.80	97.68
	51.56	2.48	15.57	10.49	0.17	4.76	9.63	3.65	1.68	96.56
	53.51	2.07	15.01	9.98	0.19	5.08	8.59	3.84	1.73	96.82
	53.93	2.07	14.82	9.53	0.17	5.15	8.75	3.78	1.80	98.27
	52.70	2.66	14.86	11.51	0.15	4.87	8.92	2.89	1.44	97.77
	51.54	2.34	15.26	10.31	0.17	4.84	9.78	3.99	1.77	97.32
	52.46	2.57	14.67	10.78	0.16	4.56	8.65	4.08	2.06	96.18
	51.82	2.49	15.28	10.39	0.19	4.70	9.65	3.81	1.68	99.28
	51.45	2.40	15.19	10.81	0.18	4.73	9.73	3.81	1.70	98.40
	51.59	2.37	14.63	10.43	0.13	5.41	10.41	3.61	1.42	98.32
	51.66	2.27	14.73	10.42	0.14	5.35	10.41	3.66	1.37	97.85
	51.80	2.26	14.82	10.15	0.15	5.33	10.48	3.59	1.41	98.28
	51.73	2.40	14.70	10.35	0.18	5.46	10.24	3.53	1.41	97.70
	51.67	2.42	15.20	10.34	0.16	4.68	9.90	3.89	1.74	97.72
	52.71	2.31	14.65	9.94	0.17	5.33	9.52	3.72	1.64	97.17
	52.88	2.25	14.86	9.86	0.17	5.34	9.11	3.94	1.59	98.11
	53.48	2.19	14.97	9.76	0.15	4.90	8.88	3.97	1.71	98.01
	53.99	2.17	14.86	9.52	0.15	4.93	8.89	3.80	1.69	96.89
	51.46	2.31	14.92	10.43	0.14	5.38	10.38	3.55	1.43	98.00
	51.58	2.45	14.77	10.06	0.16	5.37	10.49	3.64	1.47	97.86
	51.49	2.38	14.41	10.46	0.12	5.43	10.53	3.68	1.50	96.25
	52.12	2.42	15.36	10.04	0.14	4.63	9.89	3.73	1.67	96.72
	51.93	2.51	15.48	10.28	0.15	4.62	9.64	3.66	1.73	97.42
	52.42	2.46	15.41	9.75	0.14	4.50	9.46	4.15	1.70	97.81
	51.23	2.62	15.01	10.71	0.16	4.76	9.82	3.95	1.73	96.57
ML3B-G(n = 10)										
Average	51.55	2.00	13.78	10.60	0.16	6.47	10.08	2.38	0.40	
2SD	*0.44*	*0.12*	*0.28*	*0.14*	*0.06*	*0.12*	*0.20*	*0.08*	*0.08*	
Preferred value	51.40	2.13	13.60	10.90	0.17	6.59	10.50	2.40	0.39	
Uncertainty (95%)	*0.60*	*0.09*	*0.20*	*0.10*	*0.01*	*0.08*	*0.10*	*0.06*	*0.00*	

impacted on this layer (Buettner et al., 1999; Eden et al., 1996; Froggatt and Lowe, 1990; Holt et al., 2011; Lowe et al., 2008; Németh, 2010; Shane, 2005). Major and minor element analyses on the glass shards show a homogeneous composition, and no clear compositional difference was recorded within one glass shard. Data were normalised to an anhydrous basis (Pearce et al., 2014). The SiO_2 varies between 51.05 wt % - 53.99 wt %, the MgO between 4.50 wt % - 5.46 wt %, CaO 8.59 wt % - 10.53 wt %, TiO_2 2.07 wt % - 2.63 wt %, and K_2O between 1.41 wt % - 2.06 wt % (Table 1; Figs. 4 and 5). The major element composition of the glass shards from ML 708 therefore plot mainly in the field of basaltic trachyandesite and trachybasalt (Fig. 4). WDS-EPMA on plagioclase minerals shows a labradorite composition (Fig. 6, Table 2), consistent with the plagioclase phenocrysts observed within pyroclastic deposits and lava flows from the ACVF by Zhao (2010).

Glass data from Gaoshan volcano fall primarily in the field of basaltic trachyandesite on a total alkali silica diagram (TAS) and the alkali content (>6.0 wt.%) is higher than those glass shards from Moon Lake (<6.0 wt %) (Figs. 4 and 5, Table 3). When compared with the whole rock data from ACVF and NVF (>6.8 wt %), glass data from Moon Lake and proximal tephra from ACVF (<5.5 wt %) display a lower MgO content (Fig. 5). The K_2O content of glass from the ACVF offers the most diagnostic element composition for differentiating between the volcanic materials from different areas.

Radiocarbon age estimates and dating procedures for the Moon Lake sediment cores have been reported previously by Liu et al. (2010). In this study, we have calculated a Bayesian-based age model using the flexible age-depth modelling software Bacon V2.2 (Blaauw and Christen, 2011). Based on this age model, tephra ML 708 is dated to 14,757 to 13,896 cal yrs BP, with median and mean ages of c. 14,200 cal yrs BP (Fig. 2).

5. Discussion

5.1. The source of the tephra in Moon Lake

Mafic explosive eruptions have been inferred to be common in many volcanic fields in NE China, including the scoria cones, tuff rings and maars of the Arxan-Chaihe (Nemeth et al., in review),

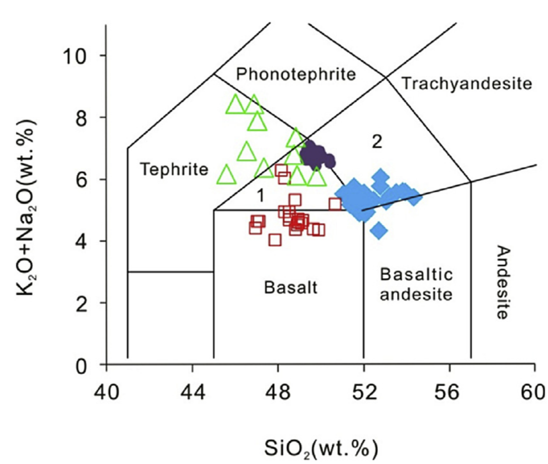

Fig. 4. TAS diagram (Le Maitre et al., 1989) for comparing the glass data from Moon Lake (blue diamonds) and Gaoshan volcano (purple circles) against the whole rock data from Nuominhe (green triangles) and Arxan-Chaihe (red squares) volcanic fields. Whole rock compositions from local Arxan – Chaihe volcanic field and Nuominhe volcanic field are from Zhao (2010). 1 = trachybasalt, 2 = basaltic trachyandesite. (For interpretation of the references to colour in this figure legend, the reader is referred to the web version of this article.)

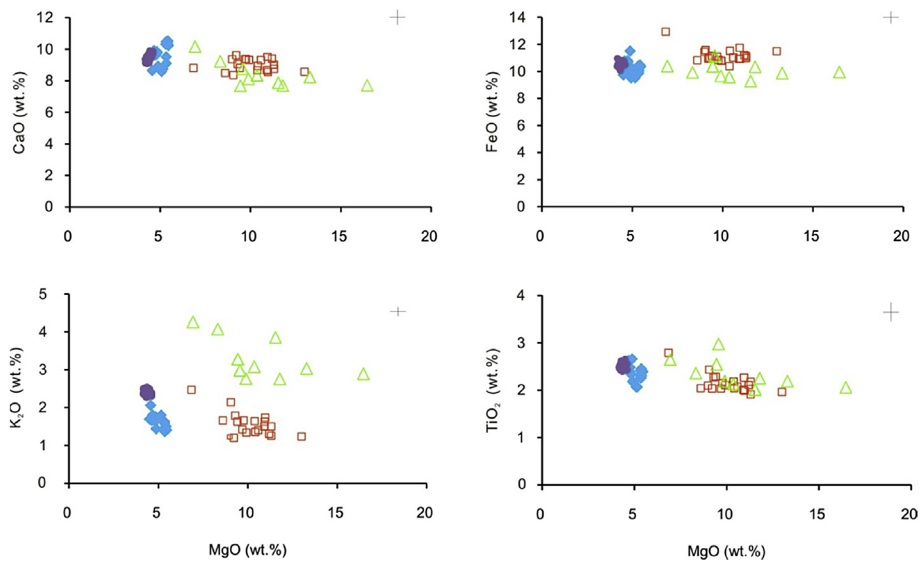

Fig. 5. Major element compositions of glass shards Moon Lake tephra ML 708 (blue diamonds) and Gaoshan volcano (purple circle) alongside the whole rock compositions from proximal Arxan – Chaihe volcanic field (red squares) and Nuominhe volcanic field (green triangle) datasets. Representative error bars (±2σ) were calculated on the basis of secondary glass standard analyses. (For interpretation of the references to colour in this figure legend, the reader is referred to the web version of this article.)

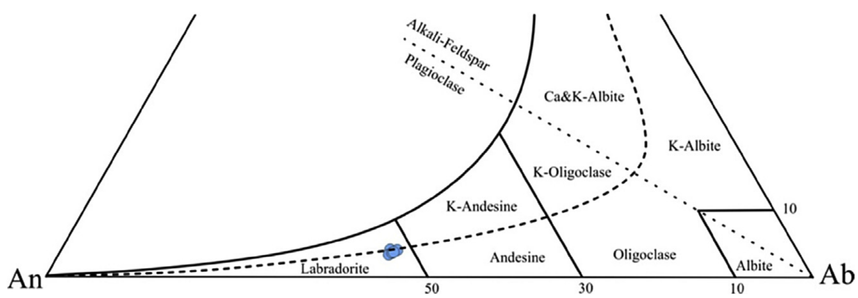

Fig. 6. Classification of plagioclase minerals from the tephra in Moon Lake. The classification of feldspar was modified from Smith and Brown (1988).

Nuominhe (Zhao, 2010), Wudalianchi (e.g. Basu et al., 1991; Hsu and Chen, 1998; Kuritani et al., 2013; Liu, 1999; McGee et al., 2015; Zou et al., 2003), Keluo (Liu, 1999), and Longgang (LGVF) volcanic fields (e.g. Fan et al., 2000, 2002; Liu et al., 2009). The presence of olivine, pyroxene and plagioclase phenocrysts within the Moon Lake tephra implies that it was probably not dispersed very far from its source. Many volcanoes within the ACVF and nearby NVF experienced explosive eruptions during the Late Pleistocene to Holocene (Zhao, 2010; Zhao et al., 2013). These locations are therefore the most likely source candidates of the newly identified tephra layer. However, volcanic centres found further afield must also be ruled-out.

In considering other possible volcanic sources in the surrounding regions, attention turns to Changbaishan volcano situated in the China–North Korea frontier. Changbaishan is a regional ash-producing stratovolcano, which has produced numerous explosive eruptions of up to VEI 7 (Horn and Schmincke, 2000) during the Late Pleistocene to Holocene. However, the eruptive products from Changbaishan are of mainly felsic composition and most of them have been transported to the east of the volcano (Chen et al., 2016; Liu et al., 2015a,b; Sun et al., 2014b, 2015). The basaltic tephra layer in Moon Lake is therefore deemed unlikely to have originated from Changbaishan volcano.

Explosive eruptions from LGVF, Wudalianchi and Jingbohu volcanic fields may also be ruled out as candidates for the origin of this basaltic tephra layer. These volcanic fields consist typically of small-to-medium volume scoria cones, with no evidence of past highly explosive activity (e.g. violent strombolian or sub-plinian eruption styles). Ash from eruptions of these volcanic fields is unlikely to have travelled more than 500 km to the ACVF, and therefore unlikely to have accumulated in a 5 mm thick layer, as seen in Moon Lake.

Table 2
Major and minor element compositions of plagioclase determined by WDS-EPMA.

	SiO_2	TiO_2	Al_2O_3	FeO	MnO	MgO	CaO	Na_2O	K_2O	Analytical total
ML 708	54.56	0.10	27.51	0.93	0.04	0.13	10.97	4.79	0.52	99.54
	54.08	0.15	27.73	0.95	0	0.12	11.22	4.69	0.54	99.48
	54.10	0.19	27.35	1.09	0	0.19	11.05	4.68	0.48	99.13
	54.08	0.19	26.87	1.08	0	0.12	10.87	4.63	0.49	98.33
	54.30	0.18	27.89	1.05	0.03	0.13	11.15	4.63	0.45	99.81

Table 3
WDS-EPMA major and minor element compositions of glass shards for the proximal tephra from ACVF. All the data have been normalised to an anhydrous basis with original analytical totals shown. MPI-DING glass standard ML3B-G was analysed to monitor the precision and accuracy of the glass data.

	SiO_2	TiO_2	Al_2O_3	FeO	MnO	MgO	CaO	Na_2O	K_2O	P_2O_5	Analytical total
Gaoshan glass	49.99	2.45	16.07	10.25	0.13	4.33	9.41	4.28	2.38	0.69	97.97
	49.47	2.62	15.99	10.58	0.18	4.29	9.09	4.65	2.44	0.68	98.33
	49.45	2.53	15.99	10.66	0.17	4.39	9.14	4.54	2.43	0.70	97.13
	50.42	2.52	15.96	10.32	0.10	4.23	9.31	4.17	2.34	0.62	96.60
	49.76	2.49	15.88	10.61	0.20	4.32	9.41	4.44	2.36	0.53	98.25
	49.36	2.51	15.96	10.43	0.23	4.24	9.53	4.53	2.42	0.78	98.36
	50.01	2.52	15.79	10.53	0.17	4.20	9.37	4.35	2.43	0.63	98.35
	49.56	2.56	15.75	10.67	0.22	4.25	9.34	4.51	2.42	0.71	98.69
	50.38	2.50	16.00	10.08	0.20	4.34	9.23	4.37	2.28	0.61	97.71
	50.05	2.40	15.74	10.46	0.20	4.35	9.39	4.36	2.37	0.68	97.52
	49.87	2.45	15.87	10.41	0.17	4.35	9.43	4.23	2.53	0.69	97.63
	49.38	2.56	15.79	10.83	0.18	4.38	9.47	4.40	2.39	0.61	98.13
	49.80	2.48	15.86	10.30	0.17	4.26	9.49	4.40	2.51	0.72	98.38
	49.83	2.42	15.81	10.43	0.13	4.26	9.50	4.46	2.33	0.83	98.44
	49.71	2.50	15.87	10.53	0.16	4.31	9.36	4.34	2.51	0.72	97.87
	49.93	2.52	15.95	10.17	0.13	4.30	9.36	4.45	2.46	0.72	99.14
	49.79	2.43	16.00	10.55	0.14	4.45	9.37	4.17	2.42	0.68	98.67
	49.65	2.62	16.00	10.62	0.12	4.31	9.34	4.32	2.40	0.63	98.43
	49.94	2.48	15.99	10.37	0.17	4.17	9.35	4.52	2.37	0.62	97.97
	49.58	2.46	15.81	10.96	0.20	4.18	9.13	4.48	2.50	0.71	97.55
	49.76	2.43	15.37	10.49	0.17	4.61	9.88	4.29	2.39	0.60	97.60
	49.77	2.56	15.71	10.49	0.15	4.61	9.70	4.11	2.32	0.58	97.70
	49.64	2.46	15.89	10.54	0.16	4.32	9.64	4.20	2.36	0.78	97.52
	49.45	2.58	15.77	10.43	0.18	4.49	9.50	4.42	2.49	0.69	98.12
	49.36	2.47	15.83	10.66	0.15	4.37	9.74	4.28	2.33	0.81	97.86
	49.25	2.50	15.72	10.62	0.20	4.42	9.90	4.38	2.42	0.58	98.23
	49.45	2.51	15.78	10.77	0.17	4.54	9.52	4.42	2.37	0.48	98.18
	49.31	2.63	15.68	10.65	0.18	4.46	9.69	4.39	2.31	0.70	98.85
	49.31	2.66	15.83	10.49	0.13	4.49	9.70	4.25	2.37	0.78	98.25
ML3B-G(n = 15)											
Average	51.83	2.06	13.55	10.92	0.16	6.32	10.34	2.41	0.39	0.23	
2SD	0.38	0.10	0.23	0.22	0.06	0.22	0.24	0.13	0.06	0.11	
Preferred value	51.40	2.13	13.60	10.90	0.17	6.59	10.50	2.40	0.39	0.23	
Uncertainty (95%)	*0.60*	*0.09*	*0.20*	*0.10*	*0.01*	*0.08*	*0.10*	*0.06*	*0.00*	*0.03*	

Evidence for explosive eruptions that generated extensive tephra sheets can also be found around the Baikal rift (Ivanov et al., 2011), but volcanic sources in that region are characterised by a higher alkali content than the ACVF volcanic. Volcanoes from the Baikal rift are also considered too far away (more than 1000 km) to have transported and deposited ash as a visible layer in Moon Lake.

Prior to this study, only whole rock analyses were available from the ACVF and NVF fields. There are offsets in composition between whole rock (WR) and *in situ* analysis on glass shards due to the inclusion of minerals and lithic fragments in the WR analyses. The fractionation of phenocrysts phases incorporates those elements compatible to them, in turn depleting the melt composition, of which glass shards are representative. This factor limits the accuracy of tephra correlations (Németh et al., 2012; Tomlinson et al., 2012) based upon different types of compositional analyses. The volcanic rocks from ACVF and NVF are of basaltic composition, and fractionation of mafic minerals increases the K_2O content of their glasses (Figs. 4 and 5). NVF rocks are potassic (Fan et al., 2015) and have a higher K_2O content than the glasses in Moon Lake tephra ML 708, which cannot be supported by the fractionation of mafic minerals. In contrast, the glass compositions of Moon Lake ML 708 tephra, have a relatively higher K_2O content than WR samples from the ACVF, which might be explained by such fractionation processes. Therefore, TAS and Harker diagrams imply that the glass compositions of Moon Lake tephra are better correlated to WR compositions from the ACVF, than to WR compositions of NVF.

The main phenocrysts reported in volcanic rocks from the ACVF are olivine and pyroxene, with additional plagioclase (Zhao, 2007). Usually, the tiny plagioclase crystals can be found as microcrysts within the glass shards (Fig. 3), which implies that they were formed not long before ejected synchronously with the volcanic eruption. Therefore, the presence of plagioclase microcrysts may also be used as an additional line of evidence to locate the source of ML 708. The chemical composition of plagioclase assemblages can also be used to correlate tephra/cryptotephra layers (Jouannic et al., 2015). The plagioclase compositions in ML 708 illustrate a labradorite member (Fig. 6), which is in line with the labradorite phenocryts reported in both lava and tephra from ACVF (Zhao, 2010). Taking into account the geochemical and mineral compositions, the tephra layer at Moon Lake is almost certainly derived from a local volcanic source within the ACVF.

Additionally, analysed glass compositions of proximal tephra from Gaoshan volcano in the ACVF do show some differences from the composition of Moon Lake tephra ML 708. In particular, the K_2O content of the glasses is distinct (Fig. 5). This implies that there is some variability in glass compositions within the ACVF, as would be expected from a volcanic field containing numerous volcanic edifices. Future investigation into the variability of melt compositions, based on detailed proximal and distal tephra sequences will give a better insight into magma evolution and petrogenesis in this region.

The volcanic rocks in the ACVF cover an area equivalent to c. 100 km^2 and comprises more than 30 individual volcanoes, all of which have poorly constrained eruption histories (Fan et al., 2011, Fig. 1). Yanshan and Gaoshan are the youngest known volcanoes. Evidence from dating of the volcanic and sedimentary sequences indicates eruptions took place in the Holocene. Radiocarbon dating of charcoal fragments buried in the pyroclastic deposits derived from Yanshan volcano yielded an age of 2000 cal yrs BP (Bai et al., 2005). Geomorphological studies reveal an absence of Holocene sediments overlying the pyroclastic sheets and lava flows around Yanshan (Bai et al., 2005; Németh et al., in review; Zhao et al., 2008); also indicative of the relative young age of the eruption. Proximal Gaoshan tephra has glass compositions more enriched in total alkalis than the Moon Lake tephra, prohibiting a direct correlation of ML 708 to the sampled material.

Volcanoes Woniupaozi and Wusulangzi (Fig. 1) were characterised by phreatomagmatic eruptions during the Pleistocene dated to c. 0.45–0.25 Ma (Fan et al., 2011), and therefore also cannot be the source of the ML 708 tephra. Xiaodonggou, Shihaopendi, Sifangshan and Zigongshan volcanoes (Fig. 1) may have had eruptions during the Holocene, but not during the Late Pleistocene; while those "highland volcanoes" near to Wusulangzi and the caldera of Arxan may have erupted during the mid-Pleistocene (Fan et al., 2011; Liu et al., 2015a; Zhao et al., 2008; Zhao, 2010). Tuofengling and other "highland volcanoes" with extensive pyroclastic sheets could also be candidates for the ML 708 tephra, as they are located only ~15 km away from Moon Lake. However, a field section at the base of Tuofengling reveals a pyroclastic succession that is covered by a lava flow dated by K-Ar dating to 0.34 ± 0.03 Ma (Chen, 2010), again excluding this centre as the source of the Moon Lake tephra.

Volcanic rocks in the broader ACVF area were produced in the same geological context. Without having extensive proximal tephra compositional data for each volcano, a direct correlation of the ML 708 cannot be made confidently to any one of the potential sources. Volcanic glass chemistry data and the general thickness/volume of the ML 708 however, enable us to suggest that it must have originated from an eruption of a nearby volcanic centre, probably not further than 50 km away from Moon Lake (Fig. 1). In order to verify the source of the Moon Lake tephra, future studies should perform detailed geochronological and geochemical studies of proximal tephra sequences from the many potentially young (post-Pleistocene) volcanoes of the ACVF.

5.2. Chronological implications

Traditional geochronological dating methods, such as Ar-Ar, K-Ar, U/Pb and radiocarbon-dating, may be challenging for many Late Pleistocene to Holocene volcanic rocks, from which it is often difficult to extract suitable mineral or organic samples. However, tephra layers recorded in lake or peat sediments may be indirectly dated by dating of the organic or inorganic materials commonly interbedded with the primary tephra layers (Molloy et al., 2009; Shane et al., 2013).

Within the ACVF, only a few Late Pleistocene to Holocene eruptions have been dated. Liu (1987), Chen (2010) and Fan et al. (2011) defined a number of Late Pleistocene effusive volcanic eruptions by K-Ar method, and as mentioned above, Bai et al. (2005) identified a Holocene explosive eruption of Yanshan by radiocarbon dating of on charcoal fragments within pyroclastic deposits (Fig. 1). Others have argued based on geomorphological and volcanic evidence, that during this period, there were also eruptions of Gaoshan, Yanshan, Shihaopendi and Xiaodonggou volcanoes (Liu, 1988, 2000), however, no direct geochronological evidence has been provided. Tephra ML 708 recorded in Moon Lake provides a new, precise age estimate, of ca. 14, 200 cal yrs BP, for a Late Pleistocene explosive eruption. Our findings imply that there were probably other as yet unnoticed and undated explosive eruptions, and suggests that tracing tephra or cryptotephra layers

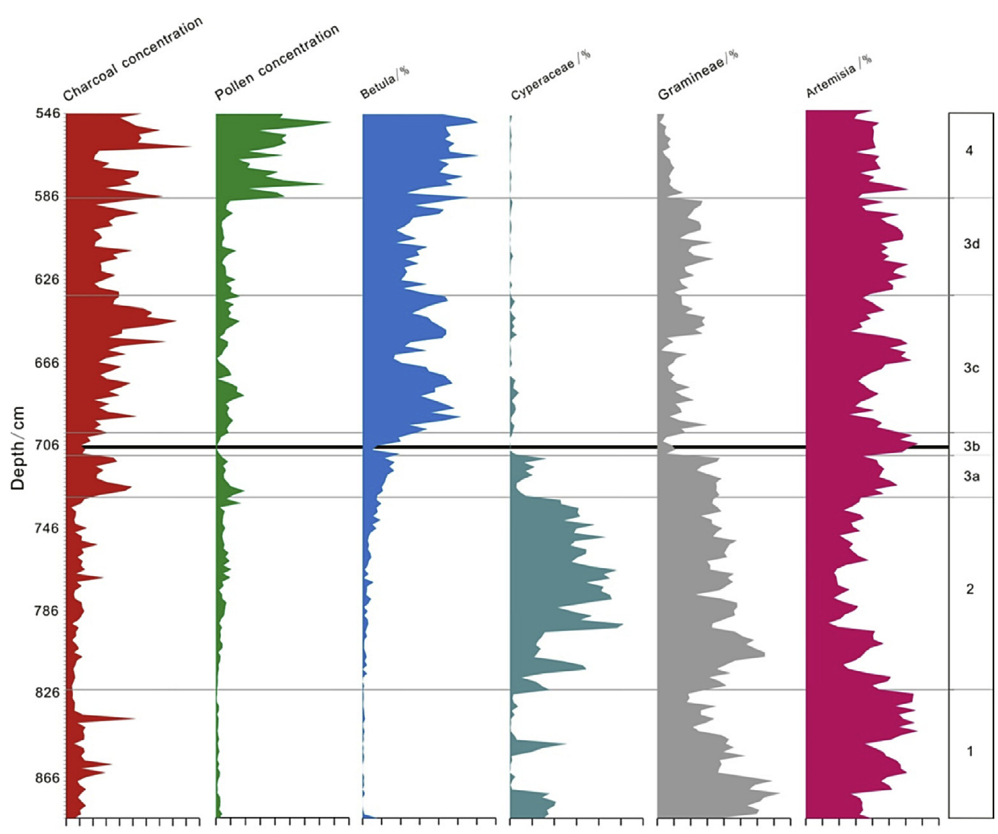

Fig. 7. Zonation of the Moon Lake sediment record based upon the pollen and charcoal records from Wu and Liu (2012, 2013). The black line at 708 cm marks the position of the tephra layer. Pollen and charcoal records suggest that the start of Late Glacial was around the boundary between 3b and 3a. Pollen and charcoal are plotted as 10^3 grains per gram.

may be an effective means to establish past volcanic activities. Identifying and distinguishing tephra and cryptotephra layers across the widely available lake and peat sediments in this region, will undoubtedly resolve many of the problems surrounding dating the Late Pleistocene to Holocene eruptions of the ACVF.

During the Late Pleistocene there were also extensive explosive eruptions in NVF, as evidenced by the presence of thick pyroclastic outcrops and larger areas of pyroclastic sheets traced across this area (Zhao, 2010; Zhao et al., 2013). Our results have shown that the NVF was not the source of the visible Late Pleistocene tephra layer in Moon Lake, suggesting that NVF eruptions may only have had significant impacts locally. Future cryptotephra studies in the sediments from the NVF will also be important in establishing a detailed regional Late Pleistocene to Holocene volcanic history. The sediments of Sifangshan Lake in NVF, for example, extend to c. 15 ka BP (Liu et al., 2015b), which identify an ideal archive to begin searching for more volcanic events.

The Late Glacial was a climatically-sensitive period characterised by increasing temperatures, overprinted by unusual and rapid climatic fluctuations. Comparing and linking these climatic events with good chronological precision is therefore very important to better understand the mechanisms of climate change (Ammann et al., 2013; Lowe, 2001; Rasmussen et al., 2014). Tephra or/and cryptotephra layers have been widely used to link records of Late Glacial climatic events in Europe (Davies et al., 2004; Lane et al., 2013a; Lowe, 2001; Matthews et al., 2011). The ML 708 tephra coincides with the beginning of the Late Glacial, or Greenland Interstadial-1 (GI-1) (Rasmussen et al., 2014), as identified from palynological studies of the Moon Lake record by Wu and Liu (2012, 2013) and shown in Fig. 7. Tephra ML 708 can therefore be used as a significant marker bed to link rapid climatic events during Late Glacial within ACVF.

6. Conclusions

This study reports, for the first time, the occurrence of a tephra layer recorded in lake sediments of the ACVF. The tephra layer and consequently the eruption have been dated to ca. 14,200 cal yrs BP, which implies that it represents a previously unknown Late Pleistocene explosive eruption in the ACVF. The compositions of glass shards and plagioclase show similar compositions to the local volcanic products of ACVF, whilst being distinct from the NVF products. Although both the ACVF and NVF share a similar geological background (Bai et al., 2012), glass compositions and documented whole rock data also suggest that the magma sources for these two fields should be different (e.g. Zhao, 2010). This tephra layer provides a first tephrochronological marker layer in the ACVF yielding a 14,200 cal yrs BP time horizon offering the potential to study sedimentary responses to the rapid climatic events during the Late Glacial across the ACVF. Our findings imply that there are likely other laterally extensive tephra/cryptotephra layers preserved in the various sedimentary records across the ACVF. Further research into these tephra layers will consequently contribute to a more detailed reconstruction of past volcanic activity in the region.

Acknowledgments

This work was supported by the National Natural Science Foundation of China (Grant Nos. 40872206, 41272392, 41572353 and 41320104006) and Chinese Post-doctoral Foundation (No. LH2015001). C. Sun would like to thank K. Jochum and B. Stoll for providing MPI-DING glasses. Huaiyu He and Zhengfu Guo (IGGCAS) were thanked for their kind suggestions on an early version of the manuscript. Sincere thanks are extended to the anonymous reviewers for their constructive comments and reviews. The Guest Editor Christine Lane was thanked for her helpful suggestions and English corrections.

References

Albert, P.G., Tomlinson, E.L., Lane, C.S., Wulf, S., Smith, V.C., Coltelli, M., Keller, J., Lo Castro, D., Manning, C.J., Müller, W., Menzies, M.A., 2013. Late glacial explosive activity on Mount Etna: implications for proximal–distal tephra correlations and the synchronisation of Mediterranean archives. J. Volcanol. Geotherm.. Res. 265 (0), 9–26.

Ammann, B., van Leeuwen, Jacqueline F.N., van der Knaap, Willem O., Lischke, H., Heiri, O., Tinner, W., 2013. Vegetation responses to rapid warming and to minor climatic fluctuations during the Late Glacial Interstadial (GI-1) at Gerzensee (Switzerland). Palaeogeogr. Palaeoclimatol. Palaeoecol. 391, 40–59. Part B.

Bai, Z., Tian, M., Wu, F., Xu, D., Li, T., 2005. Yanshan, gaoshan — two active volcanoes of the volcanic cluster in Arshan, Inner Mongolia (In Chinese with English abstract). Earthq. Res. China 21 (1), 113–117.

Bai, Z., Tan, Q., Xu, G., Xu, D., Wang, Y., 2012. Late Quaternary volcanic activity and neotectonics in the eastern Inner Mongolia (In Chinese with English abstract). Acta Petrol. Sin. 28 (4), 1099–1107.

Bao, K., 2012. Peat Deposite and its Past 200-year Records of Environmental Changes in Mountain Peatlands, Northeast China. Graduste University of Chinese Academy of Sciences, Beijing (In Chinese with English abstract).

Bao, K., Xing, W., Yu, X., Zhao, H., McLaughlin, N., Lu, X., Wang, G., 2012. Recent atmospheric dust deposition in an ombrotrophic peat bog in Great Hinggan Mountain, Northeast China. Sci. Total Environ. 431, 33–45.

Bao, K., Shen, J., Wang, G., Le Roux, G., 2015. Atmospheric deposition history of trace metals and metalloids for the last 200 years recorded by three peat cores in Great Hinggan Mountain, northeast China. Atmosphere 6 (3), 380–409.

Basu, A.R., Wang, J., Huang, W., Xie, G., Tatsumoto, M., 1991. Major element, REE, and Pb, Nd and Sr isotopic geochemistry of Cenozoic volcanic rocks of eastern China: implications for their origin from suboceanic-type mantle reservoirs. Earth Planet. Sci. Lett. 105 (1–3), 149–169.

Blaauw, M., Christen, J.A., 2011. Flexible paleoclimate age-depth models using an autoregressive gamma process. Bayesian Anal. 6, 457–474.

Buettner, R., Dellino, P., Zimanowski, B., 1999. Identifying magma-water interaction from the surface features of ash particles. Nature 401 (6754), 688–690.

Chen, X., 2010. Chronology and Geohemistry Study of Cenozoic Volcanic Rocks of Northern Great Xing'an Range, Northeast China. Graduste University of Chinese Academy of Sciences, Beijing (In Chinese with English abstract).

Chen, X., Blockley, S.P.E., Tarasov, P.E., Xu, Y., McLean, D., Tomlinson, E.L., Albert, P.G., Liu, J., Muller, S., Wagner, M., Menzies, M.A., 2016. Clarifying the distal to proximal tephrochronology of the Millennium (B-Tm) eruption, Changbaishan Volcano, northeast China. Quat. Geochronol. 33, 61–75.

Christenson, B., Németh, K., Rouwet, D., Tassi, F., Vandemeulebrouck, J., Varekamp, J.C., 2015. Volcanic lakes. In: Rouwet, D., Christenson, B., Tassi, F., Vandemeulebrouck, J. (Eds.), Volcanic Lakes. Springer-Verlag, Berlin – Heidelberg, pp. 1–20.

Coulter, S.E., Pilcher, J.R., Plunkett, G., Baillie, M., Hall, V.A., Steffensen, J.P., Vinther, B.M., Clausen, H.B., Johnsen, S.J., 2012. Holocene tephras highlight complexity of volcanic signals in Greenland ice cores. J. Geophys. Res. 117 (D21), D21303.

Davies, S.M., Wohlfarth, B., Wastegard, S., Andersson, M., Blockley, S., Possnert, G., 2004. Were there two Borrobol Tephras during the early Lateglacial period: implications for tephrochronology? Quat. Sci. Rev. 23 (5–6), 581–589.

Davies, S.M., 2015. Cryptotephras: the revolution in correlation and precision dating. J. Quat. Sci. 30 (2), 114–130.

Eden, D.N., Froggatt, P.C., Zheng, H.H., Machida, H., 1996. Volcanic glass found in late Quaternary Chinese loess: a pointer for future studies? Quat. Int. 34–6, 107–111.

Fan, Q., Gui, J., Liu, R., Wei, H., Li, N., 2000. Petrology and geochemistry of Jinlongdingzi active volcano—the most recent Basaltic explosive volcano at Longgang. Chin. J. Geochem 19 (4), 312–317.

Fan, Q., Sui, J., Liu, R., Wei, H., Li, D., Sun, Q., Li, N., 2002. Periods of Quarternary volcanic activity in Longgang area, Jilin province (In Chinese with English abstract). Acta Petrol. Sin. 18 (4), 495–500.

Fan, Q., Sui, J., Zhao, Y., Sun, Q., Li, N., Du, X., 2008. Preliminary study on garnet peridonite xenolith of Quaternary volcanic rocks in middle Daxing'an Mountain range (In Chinese with English abstract). Acta Petrol. Sin. 24 (11), 2563–2568.

Fan, Q., Zhao, Y., Li, D., Wu, Y., Sui, J., Zheng, D., 2011. Studies on Quaternary volcanism stages of Halaha river and Chaoer river area in the Great Xing'an range: evidence from K-Ar dating and volcanic geology features (In Chinese with English abstract). Acta Petrol. Sin. 27 (10), 2827–2832.

Fan, Q., Zhao, Y., Chen, S., Li, N., Sui, J., 2015. Quaternary volcanic activities in the west of the Daxing'anling-Taihangshan gravity lineament (In Chinese with English abstract). Bull. Mineral. Petrol. Geochem 34 (4), 674–681.

Froggatt, P.C., Lowe, D.J., 1990. A review of Late Quaternary silicic and some other tephra formations from New-Zealand - their stratigraphy, nomenclature, distribution, volume, and age. New Zeal. J. Geol. Geop 33 (1), 89–109.

Holt, K.A., Lowe, D.J., Hogg, A.G., Wallace, R.C., 2011. Distal occurrence of mid-Holocene Whakatane Tephra on the Chatham Islands, New Zealand, and potential for cryptotephra studies. Quat. Int. 246 (1–2), 344–351.

Horn, S., Schmincke, H.-U., 2000. Volatile emission during the eruption of

Baitoushan Volcano (China/North Korea) ca. 969 AD. Bul. Volcanol. 61 (8), 537–555.
Hsu, C.-N., Chen, J.-c., 1998. Geochemistry of late Cenozoic basalts from Wudalianchi and Jingpohu areas, Heilongjiang province, northeast China. J. Asian Earth Sci. 16 (4), 385–405.
Ivanov, A., Arzhannikov, S., Demonterova, E., Arzhannikova, A., Orlova, L., 2011. Jom-Bolok Holocene volcanic field in the East Sayan Mts., Siberia, Russia: structure, style of eruptions, magma compositions, and radiocarbon dating. Bull. Volcanol. 73 (9), 1279–1294.
Jouannic, G., Walter-Simonnet, A.-V., Bossuet, G., Begeot, C., Develle, A.-L., 2015. Feldspar composition as an efficient tool for tephra identification: a case study from Holocene and Lateglacial lacustrine sequences (Jura, France). J. Quat. Sci. 30 (6), 569–583.
Jochum, K.P., et al., 2006. MPI-DING reference glasses for in situ microanalysis: new reference values for element concentrations and isotope ratios. Geochem., Geophys., Geosyst. 7 (2), Q02008.
Kuritani, T., Kimura, J.-I., Ohtan, E., Miyamoto, H., Furuyama, K., 2013. Transition zone origin of potassic basalts from Wudalianchi volcano, northeast China. Lithos 156–159 (0), 1–12.
Lane, C.S., Andrič, M., Cullen, V., Blockley, S., 2011. The occurrence of distal Icelandic and Italian tephra in the Lateglacial of lake Bled, Slovenia. Quat. Sci. Rev. 30 (9–10), 1013–1018.
Lane, C.S., Brauer, A., Blockley, S.P.E., Dulski, P., 2013a. Volcanic ash reveals time-transgressive abrupt climate change during the Younger Dryas. Geology 41, 1251–1254.
Lane, C.S., Chorn, B.T., Johnson, T.C., 2013b. Ash from the Toba supereruption in Lake Malawi shows no volcanic winter in East Africa at 75 ka. Proc. Natl. Acad. Sci. U. S. A 110 (20), 8025–8029.
Le Maitre, R.W., Bateman, P., Dudek, A., Keller, J., Lameyre, J., Le Bas, M.J., Sabine, P.A., Schmid, R., Sorensen, H., Streckeisen, A., Woolley, A.R., Zanettin, B., 1989. A Classification of Igneous Rocks and a Glossary of Terms. Blackwell Sciencific, Oxford.
Lin, Q., Leng, X., Hong, B., 2004. The peat record of 1 ka of climate change in Daxing Anling (In Chinese with English abstract). Bull. Mineral. Petrol. Geochem 23 (1), 15–18.
Liu, Q., Li, Q., Wang, L., Chu, G., 2010. Stable carbon isotope record of bulk organic matter from a sediment core at Moon lake in the middle part of the Daxing'an Mountain range, northeast China during the last 21 ka (In Chinese with English abstract). Quat. Sci. 30 (6), 1069–1077.
Liu, J., Chu, G., Han, J., Rioual, P., Jiao, W., Wang, K., 2009. Volcanic eruptions in the Longgang volcanic field, northeastern China, during the past 15,000 years. J. Asian Earth Sci. 34 (5), 645–654.
Liu, J., 1987. Study on geochronology of the Cenozoic volcanic rocks in northeast China (In Chinese). Acta Petrol. Sin. 3 (4), 21–31.
Liu, J., 1988. The Ceonozoic volcanic episodes in northeast China (In Chinese). Acta Petrol. Sin. 4 (1), 1–10.
Liu, J., 1999. Volcano in China. Science Press, Beijing, pp. 1–219 (In Chinese).
Liu, J., Han, J., Fyfe, W., 2001. Cenozoic episodic volcanism and continental rifting in northeast China and possible link to Japan Sea development as revealed from K–Ar geochronology. Tectonophysics 339 (3–4), 385–401.
Liu, J., Chen, S., Guo, Z., Guo, W., He, H., You, H., Kim, H., Sung, G., Kim, H., 2015a. Geological background and geodynamic mechanism of Mt. Changbai volcanoes on the China–Korea border. Lithos 236–237, 46–73.
Liu, J., Liu, Q., Chu, G., Wu, J., Liu, J., 2015b. Sediment record at lake Sifangshan in the central-northen part of the Great Xing'an Range, northeast China since 15.4 ka B.P (In Chinese with English abstract). Quat. Sci. 35 (4), 901–912.
Liu, R., 2000. Active Volcanoes of China. Seismological Press, Beijing, pp. 1–93 (In Chinese).
Lowe, J.J., 2001. Abrupt climatic changes in Europe during the last glacial–interglacial transition: the potential for testing hypotheses on the synchroneity of climatic events using tephrochronology. Glob. Planet. Change 30 (1–2), 73–84.
Lowe, John, Barton, Nick, Blockley, Simon, Ramsey, Christopher Bronk, Cullen, Victoria L., Davies, William, Gamble, Clive, Grant, Katharine, Hardiman, Mark, Housley, Rupert, Lane, Christine S., Lee, Sharen, Lewis, Mark, MacLeod, Alison, Menzies, Martin, Müller, Wolfgang, Pollard, Mark, Price, Catherine, Roberts, Andrew P., Rohling, Eelco J., Satow, Chris, Smith, Victoria C., Stringer, Chris B., Tomlinson, Emma L., White, Dustin, Albert, Paul, Arienzo, Ilenia, Barker, Graeme, Borić, Dušan, Carandente, Antonio, Civetta, Lucia, Ferrier, Catherine, Guadelli, Jean-Luc, Karkanas, Panagiotis, Koumouzelis, Margarita, Müller, Ulrich C., Orsi, Giovanni, Pross, Jörg, Rosi, Mauro, Shalamanov-Korobar, Ljiljiana, Sirakov, Nikolay, Tzedakis, Polychronis C., 2012. Volcanic ash layers illuminate the resilience of Neanderthals and early modern humans to natural hazards. Proc. Natl. Acad. Sci. U. S. A 109 (34), 13532–13537.
Lowe, D.J., 2011. Tephrochronology and its application: a review. Quat. Geochronol. 6 (2), 107–153.
Lowe, D.J., Shane, P.A., Alloway, B.V., Newnham, R.M., 2008. Fingerprints and age models for widespread New Zealand tephra marker beds erupted since 30,000 years ago: a framework for NZ-INTIMATE. Quat. Sci. Rev. 27, 95–126.
McGee, L.E., McLeod, C., Davidson, J., 2015. A spectrum of disequilibrium melting preserved in lava-hosted, partially melted crustal xenoliths from the Wudalianchi volcanic field, NE China. Chem. Geol. 417, 184–199.
Matthews, I.P., Birks, H., Bourne, A., Brooks, S., Lowe, J., MacLeod, A., Pyne-O'Donnell, S., 2011. New age estimates and climatostratigraphic correlations for the Borrobol and Penifiler tephras: evidence from Abernethy forest. Scotl. J. Quat. Sci. 26 (3), 247–252.
Molloy, C., Shane, P., Augustinus, P., 2009. Eruption recurrence rates in a basaltic volcanic field based on tephra layers in maar sediments: implications for hazards in the Auckland volcanic field. Geol. Soc. Am. Bull. 121 (11–12), 1666–1677.
Németh, K., Wu, J., Sun, C., and Liu, L., Update on the volcanic geoheritage values of the Cenozoic intraplate volcanic fields of Inner Mongolia, China: the Pliocene to QuaternaryAershan/Arxan – Chaihe volcanic fields. Geoheritage, submitted for publication.
Németh, K., Cronin, S.J., Smith, I.E.M., Flores, J.A., 2012. Amplified hazard of small-volume monogenetic eruptions due to environmental controls, Orakei Basian, Auckland Volcanic Field, New Zealand. Bull. Volcanol. 74 (9), 2121–2137.
Németh, K., Cronin, S.J., 2009. Volcanic structures and oral traditions of volcanism of Western Samoa (SW Pacific) and their implications for hazard education. J. Volcanol. Geotherm. Res. 186 (3–4), 223–237.
Németh, K., 2010. Volcanic glass textures, shape characteristics and compositions of phreatomagmatic rock units from the Western Hungarian monogenetic volcanic fields and their implications for magma fragmentation. Cent. Eur. J. Geosci. 2 (3), 399–419.
Pearce, N.J.G., Westgate, J.A., Perkins, W.T., Preece, S.J., 2004a. The application of ICP-MS methods to tephrochronological problems. Appl. Geochem 19 (3), 289–322.
Pearce, N.J.G., Westgate, J.A., Preece, S.J., Eastwood, W.J., Perkins, W.T., 2004b. Identification of Aniakchak (Alaska) tephra in Greenland ice core challenges the 1645 BC date for Minoan eruption of Santorini. Geochem., Geophys., Geosyst. 5 (3), Q03005.
Pearce, N.J.G., Abbott, P.M., Martin-Jones, Catherine, 2014. Microbeam Methods for the Analysis of Glass in Fine-grained Tephra Deposits: a SMART Perspective on Current and Future Trends. Geological Society, London, pp. 29–46. Special Publications, 398.
Plunkett, G., Coulter, S.E., Ponomareva, V.V., Blaauw, M., Klimaschewski, A., Hammarlund, D., 2015. Distal tephrochronology in volcanic regions: challenges and insights from Kamchatkan lake sediments. Glob. Planet. Change 134, 26–40.
Rasmussen, Sune O., Bigler, Matthias, Blockley, Simon P., Blunier, Thomas, Buchardt, Susanne L., Clausen, Henrik B., Cvijanovic, Ivana, Dahl-Jensen, Dorthe, Johnsen, Sigfus J., Fischer, Hubertus, Gkinis, Vasileios, Guillevic, Myriam, Hoek, Wim Z., Lowe, J. John, Pedro, Joel B., Popp, Trevor, Seierstad, Inger K., Steffensen, Jørgen Peder, Svensson, Anders M., Vallelonga, Paul, Vinther, Bo M., Walker, Mike J.C., Wheatley, Joe J., Winstrup, Mai, 2014. A stratigraphic framework for abrupt climatic changes during the Last Glacial period based on three synchronized Greenland ice-core records: refining and extending the INTIMATE event stratigraphy. Quat. Sci. Rev. 106, 14–28.
Shane, P., 1998. Correlation of rhyolitic pyroclastic eruptive units from the Taupo volcanic zone by Fe-Ti oxide compositional data. Bull. Volcanol. 60 (3), 224–238.
Shane, P., 2005. Towards a comprehensive distal andesitic tephrostratigraphic framework for New Zealand based on eruptions from Egmont volcano. J. Quat. Sci. 20 (1), 45–57.
Shane, P., Nairn, I.A., Martin, S.B., Smith, V.C., 2008. Compositional heterogeneity in tephra deposits resulting from the eruption of multiple magma bodies: implications for tephrochronology. Quat. Int. 178 (1), 44–53.
Shane, P., Gehrels, M., Zawalna-Geer, A., Augustinus, P., Lindsay, J., Chaillou, I., 2013. Longevity of a small shield volcano revealed by crypto-tephra studies (Rangitoto volcano, New Zealand): change in eruptive behavior of a basaltic field. J. Volcanol. Geotherm. Res. 257, 174–183.
Smith, J.V., Brown, W.L., 1988. Feldspar Minerals. Springer-Verlag, p. 828.
Smith, V.C., Pearce, N., Matthews, N., Westgate, J., Petraglia, M., Haslam, M., Lane, C., Korisettar, R., Pal, J., 2011. Geochemical fingerprinting of the widespread Toba tephra using biotite compositions. Quat. Int. 246 (1–2), 97–104.
Sun, C., Plunkett, G., Liu, J., Zhao, H., Sigl, M., McConnell, J., Pilcher, J., Vinther, B., Steffensen, J., Hall, V., 2014a. Ash from Changbaishan Millennium eruption recorded in Greenland ice: implications for determining the eruption's timing and impact. Geophys. Res. Lett. 41 (2), 694–701.
Sun, C., You, H., Liu, J., Li, X., Gao, J., Chen, S., 2014b. Distribution, geochemistry and age of the Millennium eruptives of Changbaishan volcano, Northeast China — A review. Front. Earth Sci. 8 (2), 216–230.
Sun, C., You, H., He, H., Zhang, L., Gao, J., Guo, W., Chen, S., Mao, Q., Liu, Q., Chu, G., Liu, J., 2015. New evidence for the presence of Changbaishan Millennium eruption ash in the Longgang volcanic field, Northeast China. Gondwana Res. 28 (1), 52–60.
Sun, C., Liu, J., You, H., Chu, G., 2016. Clinopyroxene and Fe-Ti oxides for correlating the ash from Changbaishan Millennium eruption. Sci. China Earth Sci. 59 (7), 1454–1462.
Tang, J., Wang, J., Chen, X., Zhao, G., Zhan, Y., 2005. Preliminary investigation for electric conductivity structure of the crust and upper mantle beneath the Aershan volcano area (In Chinese with English abstract). Chin. J. Geophys 48 (1), 196–202.
Tomlinson, E.L., Kinvig, H., Smith, V., Blundy, J., Gottsmann, J., Muller, W., Menzies, M., 2012. The Upper and Lower Nisyros Pumices: Revisions to the Mediterranean tephrostratigraphic record based on micron-beam glass geochemistry. J. Volcanol. Geotherm. Res. 243–244 (0), 69–80.
Wu, J., Liu, Q., 2012. Pollen-recorded vegetation and climate changes from Moon lake since Late Glacial (In Chinese with English abstract). Earth Sci. J. China Univ. Geosci. 37 (5), 947–954.
Wu, J., Liu, Q., 2013. Charcoal-recorded climate changes from Moon Lake in late

glacial (In Chinese with English abstract). Chin. J. Geol. 48 (3), 860–869.
Wu, J., Liu, Q., Wang, L., Chu, G., Liu, J., 2016. Vegetation and climate change during the last deglaciation in the Great Khingan Mountain, northeastern China. Plos One 11 (1), e0146261.
Zhang, Y., Liu, X., Lin, Q., Gao, C., Wang, J., Wang, G., 2014. Vegetation and climate change over the past 800 years in the monsoon margin of northeastern China reconstructed from n-alkanes from the Great Hinggan Mountain ombrotrophic peat bog. Org. Geochem 76, 128–135.
Zhao, Y., 2007. Study on tectonic quaternary volcanoes in Arshan-Chaihe area, Inner-Mongolia (In Chinese with English abstract). China University of Geosciences (Beijing), Beijing.
Zhao, Y., 2010. Study on Geology and Geochemistry of Quaternary Volcanoes in the Da Hinggan Ling Mountains (In Chinese with English abstract). Institute of Geology, China Earthquake Administration, Beijing.
Zhao, Y., Fan, Q., 2010. Yanshan and Gaoshan volcanoes in the Daxingan Mountain range – a new eruption style (In Chinese with English abstract). Seismol. Geol. 32 (1), 28–37.
Zhao, Y., Fan, Q., Bai, Z., Sun, Q., Li, N., Sui, J., Du, X., 2008. Preliminary study on quternary volcanoes in the Halaha river and Chaoer river area in Daxing'an mountain range (In Chinese with English abstract). Acta Petrol. Sin. 24 (11), 2569–2575.
Zhao, Y., Fan, Q., 2012. Mantle sources and magma genesis of Quaternary volcanic rocks in the Halaha river and Chaoer river area, Great Xing'an range (In Chinese with English abstract). Acta Petrol. Sin. 28 (4), 1119–1129.
Zhao, Y., Fan, Q., Bai, Z., Sui, J., 2013. Quaternary volcanism in the nuomin river and Kuile river area of the greater Hinggan mountains (In Chinese with English abstract). Sci. China Earth Sci. 56, 173–181.
Zolitschka, B., Anselmetti, F., Ariztegui, D., Corbella, H., Francus, P., Lucke, A., Wastegard, S., 2013. Environment and climate of the last 51,000 years – new insights from the Potrok Aike maar lake Sediment Archive Drilling prOject (PASADO). Quat. Sci. Rev. 71, 1–12.
Zou, H., Reid, M.R., Liu, Y., Yao, Y., Xu, X., Fan, Q., 2003. Constraints on the origin of historic potassic basalts from northeast China by U–Th disequilibrium data. Chem. Geo 200 (1–2), 189–201.